# Separating Hydrocarbon Mixtures by Driving the Components in Opposite Directions: High Degree of Separation Factor and Energy Efficiency

Shubhadeep Nag[1], G. Ananthakrishna,[2] Prabal K. Maiti,[3] and Subramanian Yashonath[1]

[1]*Solid State and Structural Chemistry Unit, Indian Institute of Science, Bangalore 560 012, India*
[2]*Materials Research Center, Indian Institute of Science, Bangalore 560 012, India*
[3]*Department of Physics, Indian Institute of Science, Bangalore 560 012, India*

A radically different approach for separation of molecular mixtures is proposed. A judicious combination of levitation effect observed in zeolites with a counter intuitive Landauer blow torch effect provides driving forces for the two components of the mixture to move in opposite directions. Using nonequilibrium Monte Carlo simulations, we illustrate the efficacy of the method for separating real mixtures of both linear *n*-pentane and its branched isomer, neopentane, and linear *n*-hexane and its branched isomer, 2,2-dimethylbutane. The method yields several orders of magnitude improvement in separation factor and relative energy efficiency by using submicron zeolite column. The extremely high purity of the resulting single components makes the method best suited for green chemistry.

The ever increasing demand for energy coupled with our overdependence on fossil fuels has led to uncontrolled emission of greenhouse gasses and consequent detrimental effects on global climate. Petroleum refining industry consumes the largest amount of energy with the most commonly used fractional distillation and allied methods consuming nearly 15% of the world's energy [1–3]. Recent reports suggest that even with the best approaches for reducing greenhouse gas emissions (such as adopting energy saving methods, renewable energy, etc.), the set targets for limiting global warming would not be achieved any time sooner than 2040 [4]. To have impact sooner, there is an urgent need to discover a radically different approach to separation that can provide a high degree of energy efficiency and separation factor. Efforts in this direction, such as discovering zeolites with large pores that are useful in catalysis as well as separation, have been limited [5–8]; although, there are a few newer separation approaches proposed [9–12]. Here, we propose a method for separation of mixtures based on altogether a new conceptual framework that drives the two components in opposite directions. The idea is to combine judiciously the levitation effect reported in diffusion studies of porous crystalline solids such as zeolites [13,14] with another counter intuitive effect known as the Landauer blow torch [15,16]. Briefly, the Levitation effect refers to the maximum in the self diffusivity of a molecule whose diameter is close to the window diameter of the zeolite while the blow torch effect refers to the depression of the barrier when a hot zone is placed in between the maximum and minimum of a bistable potential, thereby facilitating surmounting the barrier.

Although levitation and blow torch (LB) effects have been used for separating an ideal mixture of Ar and Ne atoms by placing the hot zone close to the window [17], the results reported are fortuitous as shown in the Supplemental Material [18]. Indeed, effectively combining these two mechanisms to drive the components in opposite directions requires a method of choosing the host zeolite for a given mixture to be separated and determining the hot zone parameters such as the position, its width and the crystalline direction along which the hot zone should be placed. Here, we show that calculating the effective potential energy (EPE) landscape experienced by the molecules of the mixture provides a general approach for determining the hot zone parameters and validating the choice of the host zeolite. This approach is used to illustrate the efficacy of the LB method by separating the real mixture of linear hydrocarbon *n* pentane and its branched isomer, neopentane, and a mixture of *n* hexane and 2,2-dimethylbutane (22DMB). We show that the method provides several orders of magnitude improvement in separation factor and energy efficiency over conventional methods.

Zeolites are porous aluminosilicates with pore diameters comparable to molecular dimensions [19]. Molecular dynamics simulations show that self-diffusivity $D$ of a guest molecule whose diameter $(\sigma_{gg})$ is comparable to the window diameter $\sigma_w$, exhibits a pronounced maximum [13], a result confirmed by experiment [20,21]. Figure 1(a) shows a plot of diffusion constant $D$ as a function of $1/\sigma_{gg}^2$. $D$ is linearly proportional to $1/\sigma_{gg}^2$ for small $\sigma_{gg}$ (called the linear regime) while a pronounced peak is seen as $\sigma_{gg}$ approaches $\sigma_w$, called anomalous or levitating regime [14].

The anomalous peak in $D$ can be understood in terms of the mean force experienced by a guest molecule from the
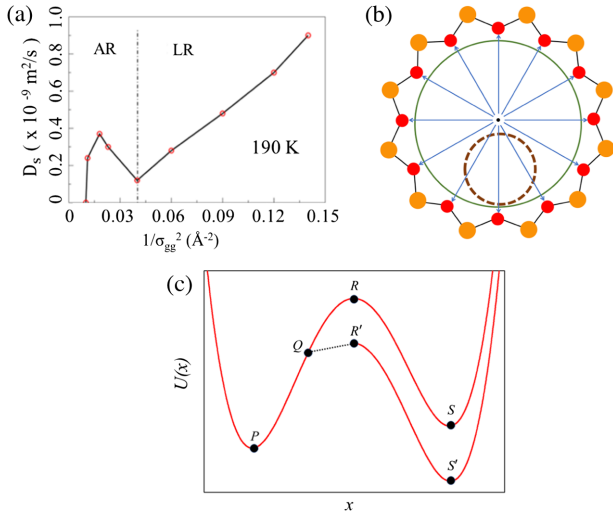
FIG. 1.   (a) Plot of self-diffusivity $D$ as a function of $1/\sigma_{gg}^2$ [13]. (b) Schematic diagram of interaction between small (dashed) and large guest (solid line) molecules with the 12-member ring. (c) The effect of placing the hot zone in the region $QR$ is to depress the higher energy minimum $S$ to $S'$.

host atoms when its size is comparable to the window size. Consider Fig. 1(b). When $\sigma_{gg} \ll \sigma_w$, the smaller guest molecule (small bold circle) is closer to the surface of the host and therefore experiences a large attractive force and a consequent smaller $D$. In contrast, the larger guest molecule (large dotted circle) for which $\sigma_{gg} \sim \sigma_w$ is nearly equidistant from opposite host surfaces resulting in smaller net force due to mutual cancellation [see Fig. 1(b)]. Therefore, the smaller particle in the linear regime experiences a maximum EPE at the window whereas the larger molecule in the anomalous regime experiences a minimum [13,14,20,21]. The resulting EPE landscape between the molecule and the host atoms depends on the precise structure of the molecules and their positions in the zeolite. A quantitative measure of these qualitative arguments is obtained by calculating the direction dependent EPE landscape. Apart from confirming the choice of the zeolite, the EPE landscapes of the two molecules allow us to determine the hot zone parameters.

In general, diffusion is an activated process. However, while diffusing through spatially heterogeneous confining medium such as zeolites, they encounter physisorption and catalytic sites that affect both static and transport properties. Reaction at such sites coupled with the poor thermal conductivity of zeolites can produce local hot zones. Then, diffusion as an activated process needs to be generalized. Landauer was the first to address the question of relative occupation probability in a bistable potential in the presence of nonuniform temperature profile [15]. For a bistable potential $U(x)$ [$PQRS$ in Fig. 1(c)] in the thermal bath of temperature $T_0$, the equilibrium population of the lower energy minimum $P$ is higher than the higher energy minimum $S$. However, if a hot zone of temperature $T_h$ is

introduced in the region $QR$ between $P$ and $R$, the occupation of the higher energy minimum $S$ can be raised above the lower energy minimum $P$, an effect called the Landauer blow torch effect. In essence, introducing a hot zone of $T = T_h$ changes the shape of the potential energy curve for the hot region $QR$ to a much flatter effective potential energy $QR'$. [To see this, inverting $P(x) \propto \exp{-U(x)/kT}$, we get $U(x)/kT = -\log P(x)$. Since $T = T_h > T_0$ in the region $QR'$, the effective potential $U(x)/kT_h$ is flatter when compared to the rest of the potential where $T = T_0$.] Since temperature elsewhere is unchanged, $P(x)$ does not change and hence the potential energy outside $QR$ remains unaltered in shape except that the point $R$ starts at $R'$ and ends at $S'$ such that the potential energy difference between $R$ and $R'$ is equal to that between $S$ and $S'$ [see Fig. 1(c)].

The topic of spatially nonuniform temperature systems have received considerable attention. Studies relevant for our problem is the development of a generalized diffusion equation in the presence of temperature and particle density gradients [22–24]. van Kampen has also shown that Onsager's transport equations relevant for the situation is the limiting case of the generalized diffusion equation [22,23,25,26]. Subsequently, increase in the escape rate on introduction of a hot zone has been demonstrated [27].

Our idea is to combine the blow torch with the levitation effect by placing the hot zone in such a way that the two components are driven in opposite directions. This can only be done by calculating the EPE landscapes of both molecules. The naive perception that the EPE of the smaller molecule has a maximum at the window does not always hold as in the case of Ar-Ne mixture (see the Supplemental Material [18]).

Zeolite NaY used in our study consists of large cages of diameter $\sim 11.4$ Å interconnected via 12-ring window (of diameter $\sim 7.4$ Å). NaY, with formula $Na_{48}Si_{144}Al_{48}O_{384}$ belongs to the cubic space group $(Fd\bar{3}m)$ with a lattice parameter $a = 24.8536$ Å [28]. A mixture of $n$ pentane (or $n$ hexane) from the linear regime and neopentane (or 22DMB) from the anomalous regime are chosen for the present Letter. The results illustrated are for $n$ pentane and neopentane mixture. The molecular dimensions of $n$-pentane and neopentane are $4.846$ by $4.154$ Å and $5.52$ by $6.74$ Å respectively. The simulation cell consists of $8 \times 1 \times 1$ unit cells of the zeolite NaY with 64 molecules each of neopentane and $n$ pentane (two guest molecules per cage). Hot zones of width 1 Å are introduced along the [100] direction [see Fig. 2(a)] in the closed intervals $[6.2134n-1.1, 6.2134n-0.1]$ Å, where $n = 1, 2, 3, \ldots, 32$. Here $6.2134$ Å is the position of 12-ring window.

Neopentane and $n$ pentane are modeled using a TraPPE united atom (UA) approach [29] with no explicit hydrogen in the calculation with one site positioned at the C atom for the groups $CH_3$, $CH_2$, and C. Our earlier computed
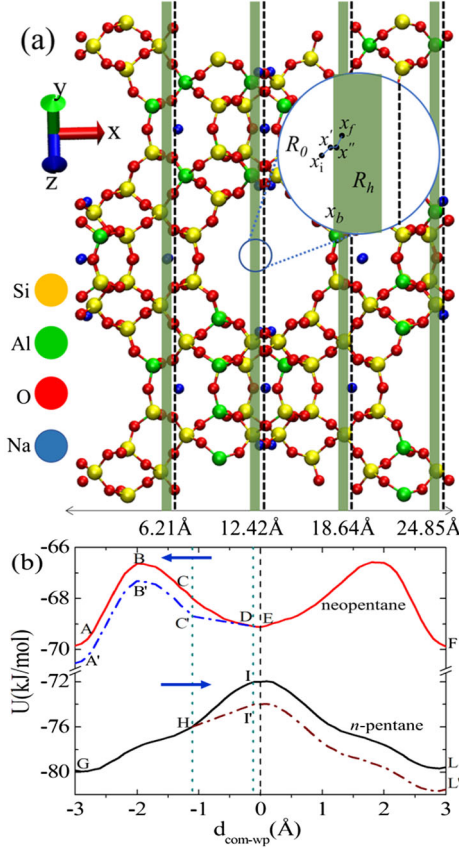
FIG. 2. (a) Zeolite NaY structure looking down the [011] direction with the window planes shown by dashed lines. Hot zones of width 1 Å (green) are shown. Inset shows ambient and hot zones, and the positions of a molecule during a Monte Carlo move. (b) The EPEs for neopentane and $n$ pentane are shown as a function of distance from the window along [111] direction. The altered EPEs of neopentane and $n$ pentane (dash-dot curves) under the influence of hot zone are also shown.

diffusivities and activation energies of pentane isomers using the UA approach are in excellent agreement with the quasi-elastic neutron scattering experiments [20,21]. See the Supplemental Material [18]. Interactions among different hydrocarbons and hydrocarbons and zeolites are represented through Lennard-Jones potential. Zeolite atoms including sodiums are modeled as flexible framework [30]. The total interaction potential $U(\vec{r})$ of the system consists of (i) host-host ($U_{hh}$), (ii) host-guest ($U_{gh}$), and (iii) guest-guest ($U_{gg}$) interaction terms. Thus, $U = U_{hh} + U_{gh} + U_{gg}$. See the Supplemental Material [18].

In our simulations, we place the hot zone slabs of width 1 Å and temperature $T_h = 330$ K periodically to the left of the window plane perpendicular to the $x$ axis as shown in Fig. 2(a). The rest of the system is maintained at $T_0 = 300$ K. The window planes of the zeolite NaY are perpendicular to the [111] direction. We have calculated the EPE landscapes for both neopentane and $n$ pentane. We find that the EPE for neopentane and $n$ pentane has a

minimum and a maximum, respectively, at the window along both [111] and [100] directions. The out-of-phase region of the EPEs of neopentane and $n$-pentane molecules are shown in Fig. 2(b). Recall that the effect of introducing a hot zone is to depress the barrier height. The altered EPEs of neopentane and $n$ pentane under the influence of the hot zone are shown by dash-dot curves in the Fig. 2(b). This drives neopentane to the left and $n$ pentane to the right. In sharp contrast, in standard methods the components of the mixture move in the same direction but at different rates with the latter determining the extent of separation.

Since we are dealing with spatially nonuniform temperature profile, we use nonequilibrium Monte Carlo (MC) simulations [31]. We use the steady state solution of van Kampen's diffusion equation [22] to obtain the transition probability from a point $x_i$ in the region $R_0$ at temperature $T_0$ to $x_f$ in the region $R_h$ at temperature $T_h$. Assuming a Markov process, diffusing across the hot zone boundary from $x_i \in R_0$ to $x_f \in R_h$ can be obtained as a sequence of three transitions from (a) $x_i \in R_0 \rightarrow x' \in [x_b - \Delta) \in R_0$, (b) $x' \in [x_b - \Delta) \in R_0 \rightarrow x'' \in [x_b + \Delta) \in R_h$, and (c) $x'' \in [x_b + \Delta) \in R_h \rightarrow x_f \in R_h$. Here $x_b$ is the ambient-hot zone boundary and $\Delta$ is a quantity that is very small. See the inset to Fig. 2(a). These are, respectively, given by

$$W_{x_i \rightarrow x'} = \min\left[1, \exp\left(-\frac{U(x_b - \Delta) - U(x_i)}{k_B T_0}\right)\right], \quad (1)$$

$$W_{x' \rightarrow x''} = \frac{T_0}{T_h}, \quad (2)$$

$$W_{x'' \rightarrow x_f} = \min\left[1, \exp\left(-\frac{U(x_f) - U(x_b + \Delta)}{k_B T_h}\right)\right]. \quad (3)$$

An expression similar to the above holds for the reverse transitions from a hot region ($R_h$) to normal region ($R_0$).

Since the two components of the mixture are driven in opposite directions, we use periodic boundary condition (PBC) along $y$ and $z$ directions and no PBC along the $x$ axis. Starting from an initial uniform distribution of $n$-pentane and neopentane molecules [see Fig. 3(a)], MC simulations were performed for $3.0 \times 10^6$ MC steps. Typical snapshots of the configurations at $0.5 \times 10^6$, $1.5 \times 10^6$, and $3.0 \times 10^6$ MC steps are shown in Figs. 3(b)–3(d). It is clear that even by $1.5 \times 10^6$ MC steps, most neopentane molecules are on the left half while $n$-pentane molecules are on the right. By $3.0 \times 10^6$ MC steps, all neopentane molecules are on the left and $n$ pentane on the right. The distribution of the densities of $n$ pentane ($n_1$) and neopentane ($n_2$) (averaged over last $1.0 \times 10^6$ steps) is shown in Fig. 4(a). Note that the density $n(x)$ exhibits peaked structure (indicating the molecules within the cages) overriding an averaged curve shown by dash-dot curves. The average curve is obtained by using a window averaging over 5 Å. The separation factor is obtained by
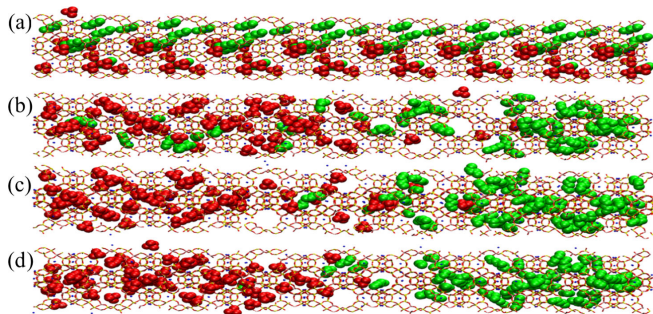
FIG. 3. (a) Initial uniformly distributed neopentane (red) and $n$ pentane (green) molecules in zeolite NaY. (b),(c),(d) show snapshots of the isomer spatial distributions at 0.5, 1.5, and $3 \times 10^6$ MC steps, respectively.

plotting the ratio of $(n_1/n_2)$ as a function of $x$ (averaged over $0.75$–$1.75 \times 10^6$ MC steps). This is shown in Fig. 4(b). It is clear that $\ln n_1/n_2$ increases linearly (dashed line) with $x$ (while $\ln n_2/n_1$ decreases, not shown) for most part of the zeolite column $l_c$. Then, one can write $n_1(x)/n_2(x) = C \exp(x/l^*)$ (or its inverse for $n_2/n_1$). Here $l^* = 18.38$ Å, and $C = 247$ for $l_c = 200$ Å. Then, the separation factor is given by $\alpha = [(n_1/n_2)|_{x=l_c}]/[(n_1/n)_2|_{x=0}] = \exp(l_c/l^*)$. For $l_c = 200$ Å used in our simulations, we get the separation factor $\alpha = 5.32 \times 10^4$. However, the expression for $n_1/n_2$ can be used to calculate $\alpha$ for longer column lengths $l_c$. Indeed, doubling $l_c$ increases $\alpha$ to $2.83 \times 10^9$. Even for $l_c = 100$ nm, $\alpha = 4.25 \times 10^{23}$. Such large $\alpha$ values have been achieved since we have used the optimized hot zone parameters such as the position and width of the hot zone determined by identifying the out-of-phase regions of the EPE landscapes of the molecules. This in turn maximizes the driving force of the two components in opposite directions.

We have calculated the energy required for separating one mole of $n$ pentane and neopentane from an equimolar
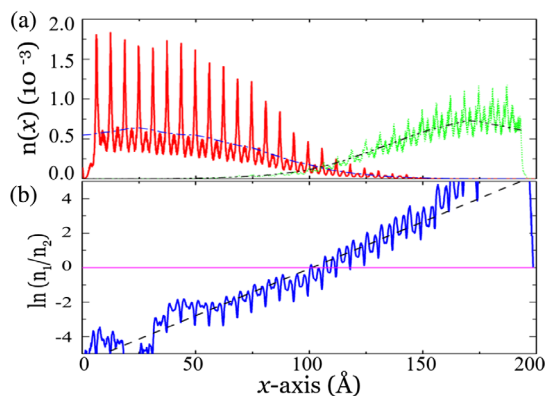


FIG. 4. (a) Density distribution for $n$ pentane (green), $n_1$ and neopentane (red), $n_2$ obtained by averaging over last $1.0 \times 10^6$ MC steps. Dashed lines show running average over 5 Å. (b) Plot of $\ln n_1/n_2$ verses length of the zeolite column.

mixture for obtaining a purity of eight 9s (99.999 999 99%) in a specified number of cycles [32,33]. We find that fractional distillation and Molex processes respectively consume $\approx 5.39 \times 10^5$ kJ/mol in $\approx 4 \times 10^5$ cycles and $\approx 5.0 \times 10^5$ kJ/mol in six cycles, respectively [34]. In comparison, our method consumes $\sim 39.42$ kJ/mol for a single cycle achieved just by using 40–100 nm long zeolite compared to several meters column length for Molex process. Thus, it is clear that the present method provides very high purity with minimum expenditure of energy in just one cycle.

Furthermore, with such a high degree of separation factor, the extremely high purity of the resulting components with no traces of other molecules are best suited for green chemistry reactions.

A mixture of $n$ hexane and 22DMB was similarly separated by first calculating EPEs of both the molecules and using it to optimize the hot zone parameters. Again, the achieved separation factor is similar to the neopentane and $n$-pentane mixture. See the Supplemental Material [18] where a snapshot at two different stages of separation is given.

We now argue that the LB effect is in principle realizable. This depends on the realizability of the two effects independently. As stated earlier, the LE has been realized in experiments [20,21]. Clearly, single crystals are best suited for diffusion of molecules in the host zeolite [35]. Since the LB process requires just a small sized crystal of length 100 nm this is not a limitation. As for producing hot zones, they can be realized in more than one way. It is possible to attach chemical groups such as $C = C$ or $C \equiv C$ (ethylene or acetylene) or $C \equiv N$ at appropriate sites between the window and cage center. These groups can be selectively excited by subjecting them to radiation of appropriate frequency. Since these are single quantum systems, the de-excitation energy has to be deposited on the local site where the chemical group is attached. This is expected to give rise to higher local temperature due to the poor thermal conductivity of zeolites. Indeed, a very similar principle has been realized in practice very recently. Tran *et al.* have demonstrated that it is possible to excite a single quantum system (color centers) from a lower to a higher vibronic level using laser over a broad range of temperatures and use it for nanoscale thermometry, although the authors do not measure the local temperature raise [36,37]. In another recent publication, the ability to manipulate, control and induce temperature changes at nanoscale has been achieved, though in gold nanorods [38]. Noting that these breakthroughs have only been achieved last year despite the huge focus on nanoscale properties for over few decades, we expect that further progress would be rapid.

The proposed LB process is a general method applicable to any binary mixture. The steps that need to be followed are these: (i) given a binary molecular mixture, a zeolite whose window diameter is comparable to the larger

molecule is chosen. (ii) The EPE landscapes for both molecules are calculated to identify the out-of-phase region. (iii) The width of the hot zone is chosen to be a finite fraction of the out-of-phase region and (iv) is placed periodically in these regions.

Finally, a few observations are in order about the generality of the LB method. First, above mentioned steps allow us to ensure good separation even when the EPE landscapes are quite complicated as in the case of neon-argon mixture (see the Supplemental Material [18]). Second, as the levitation and blow-torch effects are independent of the nature of interaction (dispersion, repulsion, and long range), our method can be used for separation of polar molecules (CO, $C_6H_5OH$, $CHCl_3$, etc.) by computing the long range interactions and the EPE landscapes. The calculated EPE are adequate for the determination of the hot zone parameters.

In summary, compared to the existing technologies for separations of linear from branched isomers, the proposed method has several major advantages such as (i) very high degree of relative energy efficiency, (ii) several orders of magnitude higher separation factor, (iii) the process requires only submicrometer length of zeolite crystals compared to 10–100 m long zeolite columns used in industries, and (iv) the extremely high purity of the resulting single components makes the present method most suited for green reactions.

[1] D. S. Sholl and R. P. Lively, Seven chemical separations to change the world, Nature (London) **532**, 435 (2016).

[2] Materials for separation technologies. Energy and emission reduction opportunities, Technical Report, Oak Ridge National Lab, ORNL, Oak Ridge, TN, United States, 2005, https://doi.org/10.2172/1218755.

[3] J. L. Humphrey and G. E. Keller, *Separation Process Technology* (McGraw-Hill, New York, 1997).

[4] C. C. Freyhardt, M. Tsapatsis, R. F. Lobo, K. J. Balkus, and M. E. Davis, A high-silica zeolite with a 14-tetrahedral-atom pore opening, Nature (London) **381**, 295 (1996).

[5] J. Susskind, G. A. Schmidt, J. N. Lee, and L. Iredell, Recent global warming as confirmed by AIRS, Environ. Res. Lett. **14**, 044030 (2019).

[6] J. M. Thomas, Design, synthesis, and in situ characterization of new solid catalysts, Angew. Chem. Int. Ed. **38**, 3588 (1999).

[7] A. H. Janssen, A. J. Koster, and K. P. de Jong, Three-dimensional transmission electron microscopic observations of mesopores in dealuminated zeolite Y, Angew. Chem. Int. Ed. **40**, 1102 (2001).

[8] J. Jiang, S. I. Sandler, M. Schenk, and B. Smit, Adsorption and separation of linear and branched alkanes on carbon nanotube bundles from configurational bias Monte Carlo simulation, Phys. Rev. B **72**, 045447 (2005).

[9] D. Banerjee, C. M. Simon, A. M. Plonka, R. K. Motkuri, J. Liu, X. Chen, B. Smit, J. B. Parise, M. Haranczyk, and P. K. Thallapally, Metal–organic framework with optimally selective xenon adsorption and separation, Nat. Commun. **7**, 11831 (2016).

[10] P. Bai, M. Y. Jeon, L. Ren, C. Knight, M. W. Deem, M. Tsapatsis, and J. I. Siepmann, Discovery of optimal zeolites for challenging separations and chemical transformations using predictive materials modelling, Nat. Commun. **6**, 5912 (2015).

[11] M. S. Shah, M. Tsapatsis, and J. I. Siepmann, Monte Carlo simulations probing the adsorptive separation of hydrogen sulfide/methane mixtures using all-silica zeolites, Langmuir **31**, 12268 (2015).

[12] H. Dong, B. Lin, K. Gilmore, T. Hou, S.-T. Lee, and Y. Li, $B_{40}$ fullerene: An efficient material for CO2 capture, storage and separation, Curr. Appl. Phys. **15**, 1084 (2015).

[13] S. Yashonath and P. Santikary, Diffusion of sorbates in zeolites Y and A: Novel dependence on sorbate size and strength of sorbate-zeolite interaction, J. Phys. Chem. **98**, 6368 (1994).

[14] S. Yashonath and P. Santikary, Diffusion in zeolites: Anomalous dependence on sorbate diameter, J. Chem. Phys. **100**, 4013 (1994).

[15] R. Landauer, Inadequacy of entropy and entropy derivatives in characterizing the steady state, Phys. Rev. A **12**, 636 (1975).

[16] A. V. Anil Kumar, S. Yashonath, and G. Ananthakrishna, Source of Reaction-Diffusion Coupling in Confined Systems due to Temperature Inhomogeneities, Phys. Rev. Lett. **88**, 120601 (2002).

[17] A. V. Anil Kumar, S. Yashonath, and G. Ananthakrishna, Separation of mixtures at nano length scales: Blow torch and levitation effect, J. Phys. Chem. B **110**, 3835 (2006).

[18] See the Supplemental Material at http://link.aps.org/supplemental/10.1103/PhysRevLett.124.255901 for the interaction potential, separation of *n*-hexane and 2,2 dimethyl butane mixture and Ne-Ar mixture are discussed.

[19] R. M. Barrer, *Hydrothermal Chemistry of Zeolites* (Academic Press, London, 1982).

[20] B. J. Borah, H. Jobic, and S. Yashonath, Levitation effect in zeolites: Quasielastic neutron scattering and molecular dynamics study of pentane isomers in zeolite NaY, J. Chem. Phys. **132**, 144507 (2010).

[21] H. Jobic, B. J. Borah, and S. Yashonath, Neutron scattering and molecular dynamics evidence for levitation effect in nanopores, J. Phys. Chem. B **113**, 12635 (2009).

[22] N. G. van Kampen, Relative stability in nonuniform temperature, IBM J. Res. Dev. **32**, 107 (1988).

[23] N. G. van Kampen, Onsager relations for transport in inhomogeneous media,, J. Stat. Phys. **63**, 1019 (1991).

[24] R. Landauer, Motion out of noisy states, J. Stat. Phys. **53**, 233 (1988).

[25] L. Onsager, Reciprocal relations in irreversible processes. I, Phys. Rev. **37**, 405 (1931).

[26] L. Onsager, Reciprocal relations in irreversible processes. II, Phys. Rev. **38,** 2265 (1931).

[27] M. Bekele, S. Rajesh, G. Ananthakrishna, and N. Kumar, Effect of Landauer's blow torch on the equilibration rate in a bistable potential, Phys. Rev. E **59,** 143 (1999).

[28] A. N. Fitch, H. Jobic, and A. Renouprez, Localization of benzene in sodium-Y-zeolite by powder neutron diffraction, J. Phys. Chem. **90,** 1311 (1986).

[29] M. G. Martin and J. I. Siepmann, Transferable potentials for phase equilibria. 1. United-atom description of *n*-Alkanes, J. Phys. Chem. B **102,** 2569 (1998).

[30] A. Gabrieli, M. Sant, P. Demontis, and G. B. Suffritti, Development and optimization of a new force field for flexible aluminosilicates, enabling fast molecular dynamics simulations on parallel architectures, J. Phys. Chem. C **117,** 503 (2013).

[31] N. Metropolis, A. W. Rosenbluth, M. N. Rosenbluth, A. H. Teller, and E. Teller, Equation of state calculations by fast computing machines, J. Chem. Phys. **21,** 1087 (1953).

[32] B. McCulloch and J. R. Lansbarkis, Honeywell UOP LLC, U.S. patent No. US5276246A (1991).

[33] G. Ananthakrishna, A. K. A. V., and S. Yashonath, Indian patent No. 1006/NAS/2001 (18, Dec, 2001); PCT patent application No. PCT/IN02/00237 (18, Dec, 2002).

[34] E. Ghasemi, S. Yazdenai, A. Rahimi, and M. Afshar, Thermodynamic evaluation of a kerosene pre-fraction unit using energy and exergy analysis, Case Stud. Thermal Eng. **10,** 413 (2017).

[35] S. Yashonath and C. Rajappa, Temperature dependence of the levitation effect Implications for separation of multi-component mixtures, Faraday Discuss. **106,** 105 (1997).

[36] T. T. Tran, B. Regan, E. A. Ekimov, Z. Mu, Y. Zhou, W. Gao, P. Narang, A. S. Solntsev, M. Toth, I. Aharonovich, and C. Bradac, Anti-Stokes excitation of solid-state quantum emitters for nanoscale thermometry, Sci. Adv. **5** (2019).

[37] P. Sehrawat, Abid, and S. S. Islam, An ultrafast quantum thermometer from graphene quantum dots, Nanoscale Adv. **1,** 1772 (2019).

[38] U. Bhattacharjee, C. A. West, S. A. Hosseini Jebeli, H. J. Goldwyn, X.-T. Kong, Z. Hu, E. K. Beutler, W.-S. Chang, K. A. Willets, S. Link, and D. J. Masiello, Active far-field control of the thermal near-field via plasmon hybridization, ACS Nano **13,** 9655 (2019).